Angular correlation of K-L x-ray cascades in gadolinium

T. Papp,[1,2] J. L. Campbell,[1] and S. Raman[3]
[1]*Guelph-Waterloo Program for Graduate Work in Physics, University of Guelph, Guelph, Ontario, Canada N1G 2W1*
[2]*Institute of Nuclear Research of the Hungarian Academy of Sciences* (ATOMKI), *Debrecen H-4001, Postfach 51, Hungary*
[3]*Oak Ridge National Laboratory, Oak Ridge, Tennessee 37831*
(Received 23 August 1993)

Angular correlation parameters (A_{22}) between the $K\alpha_1$ and L_3 x rays were measured for gadolinium in the electron-capture decay of the isotope ^{157}Tb. The results are $A_{22}(K\alpha_1\text{-}Ll)=0.272\pm0.042$, $A_{22}(K\alpha_1\text{-}L\alpha)=0.032\pm0.015$, $A_{22}(K\alpha_1\text{-}L\beta_{2,15})=0.061\pm0.018$. These values are in very good agreement with the theoretical calculations of Scofield [Lawrence Livermore Laboratory Report No. UCRL 51231, 1972 (unpublished)]; however, they differ from the earlier experimental data for the $K\alpha_1$-Ll cascade in the $60<Z<70$ atomic-number region.

PACS number(s): 32.30.Rj, 32.80.Hd

I. INTRODUCTION

The results of various experimental measurements of the angular correlations between K and L_3 x rays were collected and compared with theoretical predictions by Macias and Zalutsky [1]. While there is fair agreement over a broad range of atomic number ($60<Z<92$) for the $K\alpha_1$-$L\alpha$ cascade, there is significant disagreement for the $K\alpha_1$-Ll case.

These apparently conflicting results were obtained by energy-dispersive x-ray spectroscopy using Si(Li) and Ge or Ge(Li) detectors. Energy-dispersive x-ray spectra are used widely in different areas of atomic and nuclear physics and in applications [2], and the accuracy of experimental results often reflects to a large degree the accuracy with which these spectra can be analyzed to provide the intensities of the various x-ray lines. Technically, angular distribution and angular correlation measurements, which involve relative quantities, are simpler than measurements of absolute quantities. An example of the latter is x-ray production cross sections by particle and photon beams; results in this area exhibit considerable scatter [3], in part due to the need for various correction factors such as detector efficiency, absorptions, etc., which are only required in a relative sense in angular distribution work.

For x-ray transitions in medium-Z elements the magnetic quadrupole ($M2$) mixing into the electric dipole ($E1$) is small and the angular correlation for the $K\alpha_1$-Ll case is a large effect [4]. The theoretical A_{22} angular correlation parameter [4] is 0.27, which produces a 40% change in the Ll x-ray yields between observation angles of 90° and 180°. On the other hand, good agreement between experiment and theory was found for the $K\alpha_1$-$L\alpha_{1,2}$ transitions, where the A_{22} parameter has the much smaller value of 0.03. The deviation for the $K\alpha_1$-Ll case, which should be straightforward to measure, is therefore surprising. However, the same deviation was observed for the anisotropy parameter ratios of the Ll and $L\alpha$ transitions in proton-impact experiments [5]. It is our opinion that the long-standing deviation for the $K\alpha_1$-Ll case needs to be understood because it has significant consequences. For example, it may limit the accuracy of the f_{23} Coster-Kronig transition probability determined with the same x-ray coincidence technique [6]. If it originates from the experimental technique or from spectrum analysis it may appear similarly in inner-shell alignment studies. On the other hand, the possibility that it is a physical effect cannot be excluded. The Ll transition has special features; the L_3 and M_1 states are strongly correlated [7], and the M_1 vacancy is filled predominantly (97%) via Coster-Kronig or super-Coster-Kronig transitions [8]; the single-particle model has not been successful in predicting the M_1 level width [9].

During the past two decades, there have been improvements in the experimental technique and the spectrum analysis, providing an ability to repeat previous angular correlation measurements with an expectation of better accuracy. We have recently reported a measurement [10] for uranium. However, the deviation of interest [1] is most pronounced in the atomic-number region between 60 and 70. We have therefore carried out an angular correlation study for gadolinium using a ^{157}Tb radioactive source.

II. EXPERIMENT

To provide gadolinium x rays, a 180-μCi $^{157}_{65}$Tb source that decays to $^{157}_{64}$Gd was prepared at the Oak Ridge National Laboratory. The method of producing ^{157}Tb has been described previously [11]. The source was deposited on a 152-μm-thick aluminum foil and it was covered with a 50-μm beryllium foil. The source diameter was determined by scanning the source with a Si(Li) detector equipped with a 0.2-mm collimator; it was less than 1 mm.

Two detectors viewed the target. The first was a Si(Li) detector manufactured by Link Analytical Plc., which was used to detect the L x rays. This Si(Li) detector has a crystal with a nominal thickness of 3 mm and it is equipped with an internal collimator which restricts its

effective diameter to 5 mm. An additional external collimator, 3 mm in diameter, was used to further restrict the x rays to the central region of the detector area. This detector has a 0.025-mm-thick Be window and an energy resolution at 5.9 keV of 133 eV [full width at half maximum (FWHM)]. The K x rays were detected by the second detector, a high-purity germanium (HPGe) detector fabricated by Aptec, Inc. It had a crystal thickness of 10 mm and a diameter of 20 mm. It is equipped with a 0.5-mm-thick Be window of unusually large diameter, 75 mm, which forms the entire front face of the cryostat, thus minimizing the scattering of K x rays which produce degraded events in the spectrum. The FWHM was 530 eV at 122 keV energy. The detector-to-source distances were 5.0 and 3.0 cm for the Si(Li) and the HPGe detectors, respectively. An aluminum absorber of thickness 0.25 mm was placed in front of the HPGe detector to block the L x rays. These two detectors were chosen for their excellent line-shape characteristics, which, in each case, have been discussed elsewhere [6,12].

Measurements were carried out at five angles (90°, 95°, 125°, 145°, and 180°), and repeated at 125° and 180°. The measurement time at each angle was three weeks, and during the 4.5-month measurement period, several spectra were collected in singles mode to check the stability of the electronic system. The electronic coincidence system is described in [10], and all the coincidence events were stored on disk in list mode (K event, L event, time). Digital stabilizers were used for the K and L spectra.

III. DATA EVALUATION

The coincidence spectra were generated by a "playback" program from the list-mode data using user-defined windows on the K x-ray, L x-ray, and time events. In every case, three windows were applied on the time spectrum to obtain the real and random coincidences. The random windows, one on each side of the time peak, had a width of half the size of the window on the peak. First the L spectra in coincidence with the $K\alpha_2$ peak were generated and fitted, and the number of counts in the $L\beta_1$ peak were determined. These $K\alpha_2$-$L\beta_1$ coincidence events, which are expected to be isotropic, were used for normalization. Although the $K\alpha_2$ and $K\alpha_1$ peaks are partially overlapping, the $L\beta_1$ peak does not overlap with any L_3 x rays; therefore the $K\alpha_2$-$L\beta_1$ events were free of window contamination. In the next step a window was established on the $K\alpha_1$ peak, as shown in Fig. 1. The $K\alpha_1$ window is represented by the shaded region in the inset. The right-hand side of the window was established at one-tenth maximum, while the left-hand side was established at one-fourth maximum. Our aim was to study the angular correlation parameters, and here it is important to minimize the window contaminations. Later, we will return to this point when the correction factor for the window contamination will be determined.

A typical L_3 spectrum obtained after random subtraction is presented in Fig. 2. The spectrum was fitted with nine peaks (five peaks for the five L_3M_i transitions, and four peaks for the L_3N_1, $L_3N_{4,5}$, L_3O_1 and $L_3O_{4,5}$ transitions). The Si(Li) detector response function was

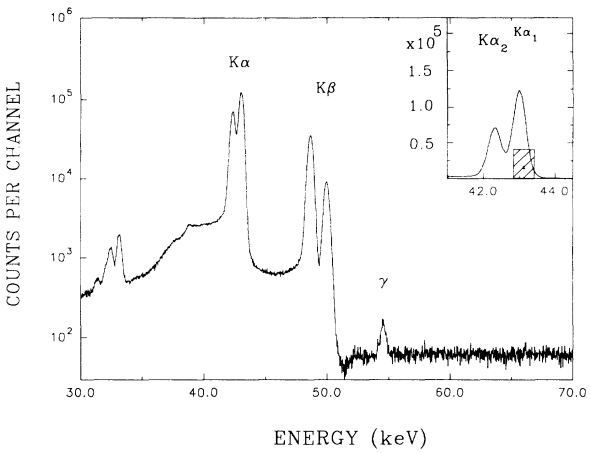

FIG. 1. K x-ray singles spectrum of gadolinium. The window used to identify the L_3 vacancies and to process the coincidence data is indicated by the shaded region in the inset.

modeled as a Gaussian peak with a tail function at the low-energy side. The tail function, which has been described in earlier studies [12], consists of a flat plateau, a short step, and a quasiexponential tailing feature whose two parameters are variables of the fit. The weaker electric-dipole-forbidden transitions were represented by this detector response function. The stronger dipole-allowed transitions were represented by the detector response function convoluted by a Lorentzian distribution representing the intrinsic distribution of x-ray energies within a given line. The spectra obtained at the different angles were first summed and fitted as a whole to determine the tail-parameter values. These values were then used as fixed parameters in the fitting of the spectra measured at different angles. It was necessary to determine the tail parameters in this way, because the individual spectra did not have large enough statistics to fit the tail parameters reliably. The background was taken to be linear and the values for the Lorentzian width of Ref. [13] were used, namely: Ll, 15 eV; $L\alpha_2$, 5 eV; $L\alpha_1$, 5 eV;

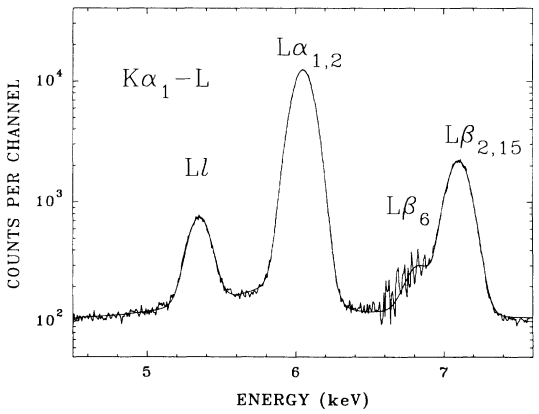

FIG. 2. Gadolinium L_3 x-ray spectrum recorded in coincidence with $K\alpha_1$ x rays. The continuous curve represents the result of the best fit.

$L\beta_{2,15}$, 5.4 eV. A weighted-least-squares fitting code [14] was then used to determine the peak areas and errors.

Because the $K\alpha_2$ and $K\alpha_1$ peaks are partially overlapping, it is important to determine the $K\alpha_2$ peak contribution to the $K\alpha_1$ window. A $K\alpha_2$ peak of low intensity will be present because L_3 x rays can be in coincidence with the $K\alpha_2$ x rays when the L_3 vacancy is created via L_2-L_3 vacancy transfer by Coster-Kronig processes. These coincidences will add an isotropic contribution to the angular correlation of the $K\alpha_1$-L_3 cascades. To take this effect into consideration, the following procedure was carried out at every angle. The playback procedure was repeated, but the windows were established on the peaks of the L spectrum, with the corresponding K spectra then being generated. Two sets of K spectra were generated in coincidence with the Ll and $L\alpha$ peaks, respectively. The windows for the Ll and $L\alpha$ peaks were set at one-hundredth maximum. The spectrum in coincidence with $L\alpha$ is shown in Fig. 3. The K spectra from the Ge detector were fitted with two peaks and a linear background. Each K x-ray peak was represented by a Lorentzian shape convoluted with the detector response function, which contained a Gaussian, a flat shelf, and an exponential tail. To determine the tail parameters a K spectrum was generated in coincidence with the $L\gamma_2(L_2$-$N_4)$ peak. This spectrum, as expected, contained only the $K\alpha_2$ peak. After we analyzed this spectrum, we determined the plateau height and the two parameters of the exponential tail. The same parameters were used for the $K\alpha_1$ peak. This approximation can be justified because the tail parameters are slowly varying with x-ray energy and the $K\alpha_2$ and $K\alpha_1$ are close in energy (indeed they are not fully resolved). With these tail parameters, the $K\alpha_1$ and $K\alpha_2$ peaks of the K spectra in coincidence with the Ll and $L\alpha$ peaks were analyzed, and the fitted areas between the windows were determined for the $K\alpha_2$ and $K\alpha_1$ peaks. In this way the isotropic contribution to the events in coincidence with the $K\alpha_2$ transition was determined, and the Ll (or $L\alpha$) peak intensities were corrected for it in the original analysis. This correction turned out to be on the order of 1%. A separate analysis was not carried out for the $L\beta_{2,15}$ peak complex; instead, we as-

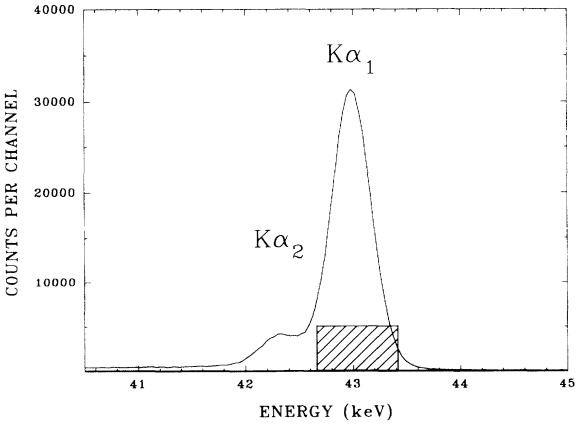

FIG. 3. Gadolinium K x-ray spectrum in coincidence with the $L\alpha$ x rays. The shaded region represents the same window as in Fig. 1, and it was used in a different playback to generate the L_3 x rays in coincidence with the $K\alpha_1$ radiation. This figure demonstrates that the window contamination is small, and it was corrected for in the analysis.

TABLE I. Angular correlation parameters (A_{22}) for the $K\alpha$-Lx cascades of Gd. The transition on which the window was set in the playback is quoted first, while the second transition quoted is the one that was fitted to determine the peak intensity. The number of coincidence events was normalized to the $K\alpha_2$-$L\beta_1$ isotropic coincidences. The β_{22} values refer to angular correlation parameters that were obtained without applying a correction for the contamination of the $K\alpha_1$ window.

Transition	β_{22}	A_{22}	Theory[a]
$K\alpha_1$-$L\alpha$	0.032±0.015	0.032±0.015	0.031
$L\alpha$-$K\alpha_1$	0.034±0.016	0.034±0.016	0.031
$K\alpha_1$-Ll	0.270±0.048	0.272±0.042	0.276
Ll-$K\alpha_1$	0.212±0.038	0.270±0.037	0.276
$K\alpha_1$-$L\beta_{2,15}$	0.061±0.018	0.061±0.018	0.047

[a]Dirac-Hartree-Slater calculation of Ref. [4].

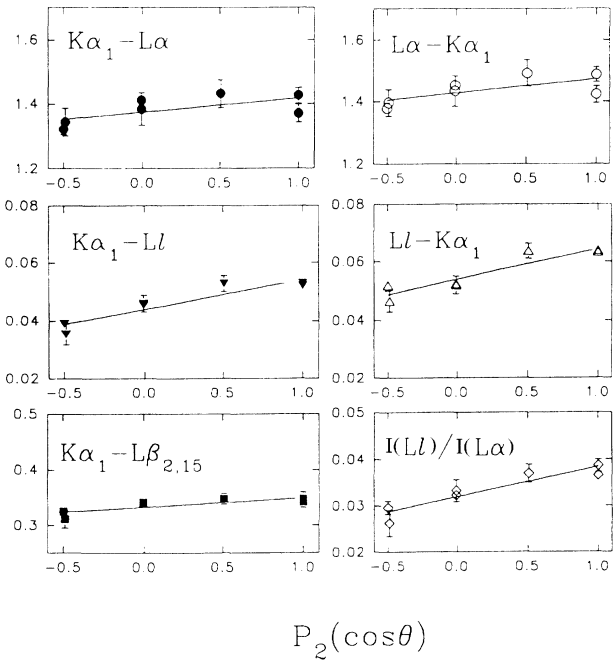

FIG. 4. The results of the angular correlation measurement for the $K\alpha_1$-Lx cascades of Gd. The transition on which the window was set in the playback is quoted first, while the second transition quoted is the one that was fitted to determine the peak intensity. The first column of graphs is the result of the analysis in which the window was set on the $K\alpha_1$ x rays and the L spectra were fitted. The two upper graphs of the right-hand column were obtained by analyzing the K spectra in coincidence with the Ll and $L\alpha$ radiation, respectively. The number of coincidence events was normalized to the $K\alpha_2$-$L\beta_1$ coincidences. The intensity ratios of the Ll and $L\alpha$ transitions are presented in the lower graph of the right-hand column, which was obtained by analyzing the L spectra in coincidence with the $K\alpha_1$ radiation.

sumed the same correction as for the $L\alpha$ transition.

The corrected intensities were normalized to the number of $K\alpha_2$-$L\beta_1$ coincidence events. The normalized intensities were fitted by a weighted-least-square procedure to an expression of the form

$$W(\theta)=W_0(1+A_{22}P_2(\cos\theta)) , \quad (1)$$

where $W(\theta)$ is the normalized intensity at the angle θ, W_0 and A_{22} are parameters of the fit, the $P_2(\cos\theta)$ is the second-order Legendre polynomial. We also fitted the angular distribution when the correction for the window contamination was not applied, and these results (denoted by β_{22}) along with the A_{22} values are shown in Table I.

Up to this point in the analysis, the approach has been to establish windows on the time spectrum and on the K spectrum to generate an L spectrum for analysis. To decide on the window contamination in the K spectrum, we generated K spectra in coincidence with the peaks of the L_3 spectrum. Obviously the opposite procedure can also be followed, where the windows are applied on the time and L spectra and the K spectra are generated, for instance, in coincidence with the Ll transition. The K spectra are then analyzed. In our case this approach might seem more appropriate at first glance because the L spectrum has much better resolution than the K spectrum (see Figs. 1 and 2). In addition, establishing windows is more straightforward on the better-resolved spectrum, but the fitting procedure is more necessary for the poorly resolved spectra. Therefore we repeated the analysis in this way. Windows were set on the Ll (or the $L\alpha$) peak and the K spectra were generated and fitted. The normalized intensities are shown in the right-hand side graphs in Fig. 4. We also repeated the determination of the corrections for the window contaminations.

In this second approach, the $L\alpha$ correction was very small. The correction for the Ll transition, however, averaged 25%. This large correction is due to the intensity differences between the Ll and $L\alpha$ transitions, and the fact that the Ll peak, as is shown in Fig. 2, is positioned on the tail of the $L\alpha$ peak. The window contamination of the Ll transition by the $L\alpha$ tail explains the differences between the uncorrected angular correlation parameters (β_{22}) of the $K\alpha_1$-Ll cascades determined by the two approaches in Table I.

There is another possibility to check the internal consistency of the analysis. The ratio of the Ll and $L\alpha$ intensities in coincidence with the $K\alpha_1$ transition has the angular correlation described by the corresponding ratio of the form given by Eq. (1). Since the $L\alpha$ transition has very small angular correlation, the angular correlation of the Ll-$L\alpha$ ratio, i.e.,

$$W(\theta)=\frac{W_0(Ll)[1+A_{22}(K\alpha_1\text{-}Ll)P_2(\cos\theta)]}{W_0(L\alpha)[1+A_{22}(K\alpha_1\text{-}L\alpha)P_2(\cos\theta)]} , \quad (2)$$

can be approximated by the function

$$W_0\left[\frac{Ll}{L\alpha}\right]\{1+[A_{22}(K\alpha_1\text{-}Ll) - A_{22}(K\alpha_1\text{-}L\alpha)]P_2(\cos\theta)\} . \quad (3)$$

When the angular dependence of the Ll-$L\alpha$ intensity ratio was fitted with this function, the A_{22} value was determined as 0.237 ± 0.041, which is in good agreement with the difference in measured angular correlation coefficients for the two transitions involved.

IV. RESULTS AND DISCUSSION

The angular correlation parameters (A_{22}) obtained in this experiment are presented in Table I and Fig. 4. The window (see first column of the table) was set on the first transition indicated, and the fitting procedure was applied to the spectrum containing the second transition. Our results are in good agreement with the theoretical values [4] for both the $K\alpha_1$-Ll and $K\alpha_1$-$L\alpha$ transitions. In contrast, the earlier experimental values [1] for the A_{22} parameter for the $K\alpha_1$-Ll cascade fell some 30–40 % below theory in the $60<Z<70$ atomic-number range. In the current work the determination of peak areas and window contamination were treated differently, using better detectors and more sophisticated fitting techniques than were available to earlier workers. After an interval of nearly two decades it is gratifying that the measured angular correlation parameters for the K-L x-ray cascades are finally in very good agreement with theory.

ACKNOWLEDGMENTS

The current work was supported in part by the Natural Sciences and Engineering Research Council of Canada and in part by the U. S. Department of Energy under Contract No. DE-AC05-84OR21400 with Martin Marietta Energy Systems, Inc. We thank A. Prindle of the Lawrence Livermore Laboratory and A. L. Beets of the Oak Ridge National Laboratory for their assistance in the initial and final preparation of the ^{157}Tb source used in this study.

[1] E. S. Macias and M. R. Zalutsky, Phys. Rev. A **9**, 2356 (1974), and references therein; Chr. Bargholtz, J. Becker, S. Beshai, M. El-khosht, K. Fransson, and B. Sundtrom, Phys. Rev. C **21**, 1078 (1980); Chr. Bargholtz, L. Homberg, and P. E. Tegner, Z. Phys. A **328**, 301 (1987).

[2] N. A. Dyson, *X-Rays in Atomic and Nuclear Physics*, 2nd ed. (Cambridge University Press, Cambridge, England, 1990).

[3] I. Orlic, C. H. Show, K. K. Loh, and S. M. Tang, At. Data Nucl. Data Tables (to be published).

[4] J. H. Scofield, Lawrence Livermore Laboratory Report No. UCRL 512 31, 1972 (unpublished); in *Atomic Inner-Shell Processes*, edited by B. Crasemann (Academic, New York, 1975), p. 265.

[5] T. Papp, Y. Awaya, A. Hitachi, T. Kambara, Y. Kanai, T. Mizogawa, and I. Torok, J. Phys. B **24**, 3797 (1991).

[6] P. L. McGhee and J. L. Campbell, J. Phys. B **21**, 2295 (1988); A. L. Catz, Phys. Rev. A **40**, 4977 (1989).

[7] A. W. Weiss, in *Beam-Foil Spectroscopy,* edited by I. A. Sellin and D. J. Pegg (Plenum, New York, 1976), p. 51.
[8] W. Bambynek, B. Crasemann, R. W. Fink, H. U. Freund, H. Mark, C. D. Swift, R. E. Price, and P. Venugopala Rao, Rev. Mod. Phys. **44**, 716 (1972).
[9] T. Papp, J. L. Campbell, J. A. Maxwell, J.-X. Wang, and W. J. Teesdale, Phys. Rev. A **45**, 1711 (1992).
[10] T. Papp, J. A. Maxwell, and J. L. Campbell, Phys. Rev. A **47**, 333 (1993).
[11] S. Raman, J. L. Campbell, A. Prindle, R. Gunnink, and J. C. Palathingal, Phys. Rev. C **46**, 2241 (1992).
[12] J. L. Campbell and J. X. Wang, X-Ray Spectrom. **20**, 191 (1991).
[13] M. A. Blokhin and I. G. Svejcer, *Handbook of X-Ray Spectroscopy* (Nauka, Moscow, 1982).
[14] J. A. Maxwell, J. L. Campbell, and W. J. Teesdale, Nucl. Instrum. Methods Phys. Res. Sect. B **43**, 218 (1989).